analytical chemistry

Article

pubs.acs.org/ac

Surface-Induced Dissociation of Protein Complexes in a Hybrid Fourier Transform Ion Cyclotron Resonance Mass Spectrometer

Jing Yan,[†] Mowei Zhou,[‡] Joshua D. Gilbert,[†] Jeremy J. Wolff,[§] Árpád Somogyi,[∥] Randall E. Pedder,[⊥] Royston S. Quintyn,[†] Lindsay J. Morrison,[†] Michael L. Easterling,[§] Ljiljana Paša-Tolić,[‡] and Vicki H. Wysocki*[,†]

[†]Department of Chemistry and Biochemistry, The Ohio State University, Columbus, Ohio 43210, United States

[‡]Environmental Molecular Sciences Laboratory, Pacific Northwest National Laboratory, Richland, Washington 99354, United States

[§]Bruker Corp., Billerica, Massachusetts 01821, United States

[∥]OSU Mass Spectrometry and Proteomics Facility, The Ohio State University, Columbus, Ohio 43210, United States

[⊥]Ardara Technologies L.P., Ardara, Pennsylvania 15615, United States

Supporting Information

ABSTRACT: Mass spectrometry continues to develop as a valuable tool in the analysis of proteins and protein complexes. In protein complex mass spectrometry studies, surface-induced dissociation (SID) has been successfully applied in quadrupole time-of-flight (Q-TOF) instruments. SID provides structural information on noncovalent protein complexes that is complementary to other techniques. However, the mass resolution of Q-TOF instruments can limit the information that can be obtained for protein complexes by SID. Fourier transform ion cyclotron resonance mass spectrometry (FT-ICR MS) provides ultrahigh resolution and ultrahigh mass accuracy measurements. In this study, an SID device was designed and successfully installed in a hybrid FT-ICR instrument in place of the standard gas collision cell. The SID-FT-ICR platform has been tested with several protein complex systems (homooligomers, a heterooligomer, and a protein−ligand complex, ranging from 53 to 85 kDa), and the results are consistent with data previously acquired on Q-TOF platforms, matching predictions from known protein interface information. SID fragments with the same m/z but different charge states are well-resolved based on distinct spacing between adjacent isotope peaks, and the addition of metal cations and ligands can also be isotopically resolved with the ultrahigh mass resolution available in FT-ICR.

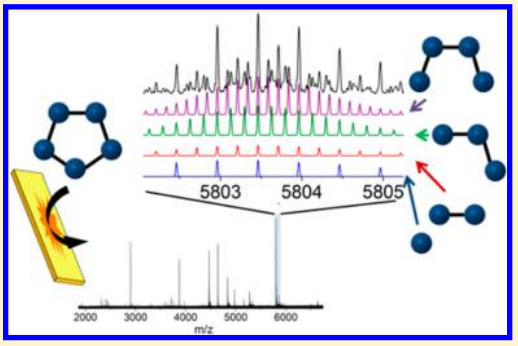

Protein complexes are involved in many cellular processes[1] and thus the study of protein interactions is essential for understanding biological processes.[2] Native mass spectrometry has become a useful tool that provides stoichiometry and quaternary structure of macromolecular complexes.[3−5] Tandem mass spectrometry with various activation methods, such as collision induced dissociation (CID),[6] electron transfer dissociation (ETD),[7] electron capture dissociation (ECD),[8] surface-induced dissociation (SID),[9] or ultraviolet photodissociation (UVPD)[10,11] have been shown to be able to provide further structural information on protein complexes. For example, the ejection of an unfolded monomer subunit from protein complexes in CID provides the stoichiometry of macromolecues.[12] ECD and ETD allow surface mapping of protein complexes by providing backbone cleavage.[7,8,13] UVPD produces both covalent and noncovalent fragments of protein complexes, providing both secondary and quaternary structure information.[10,11] SID has been shown to produce noncovalent subcomplex fragments with symmetric charge partitioning indicating the relative strength of interfaces for many protein complexes, which provide insight into the quaternary structure of protein complexes.[14] The conformational changes of protein complexes can also been monitored by SID.[15] SID was successfully implemented in quadrupole time-of-flight (Q-TOF) instruments.[16] Coupling with ion mobility provides additional separation in Q-TOF instruments, that is, fragments with the same m/z can be differentiated based on drift time.[17] However, the mass resolution of Q-TOF instruments sometimes limits the information that is obtained for protein complexes by SID when systems with minor mass differences, such as protein modifications and ligand binding, are studied.[14]

Fourier transform ion cyclotron resonance mass spectrometry (FT-ICR MS) provides m/z measurements with ultrahigh resolution and ultrahigh mass accuracy.[18] The development of the ParaCell mass analyzer made it possible to improve the collection of long transients that are necessary for protein complex studies.[8,19,20] Previous studies have shown that large protein complexes up to 186 kDa can be isotopically resolved in

Received: October 10, 2016
Accepted: December 2, 2016
Published: December 2, 2016

DOI: 10.1021/acs.analchem.6b03986
Anal. Chem. 2017, 89, 895−901

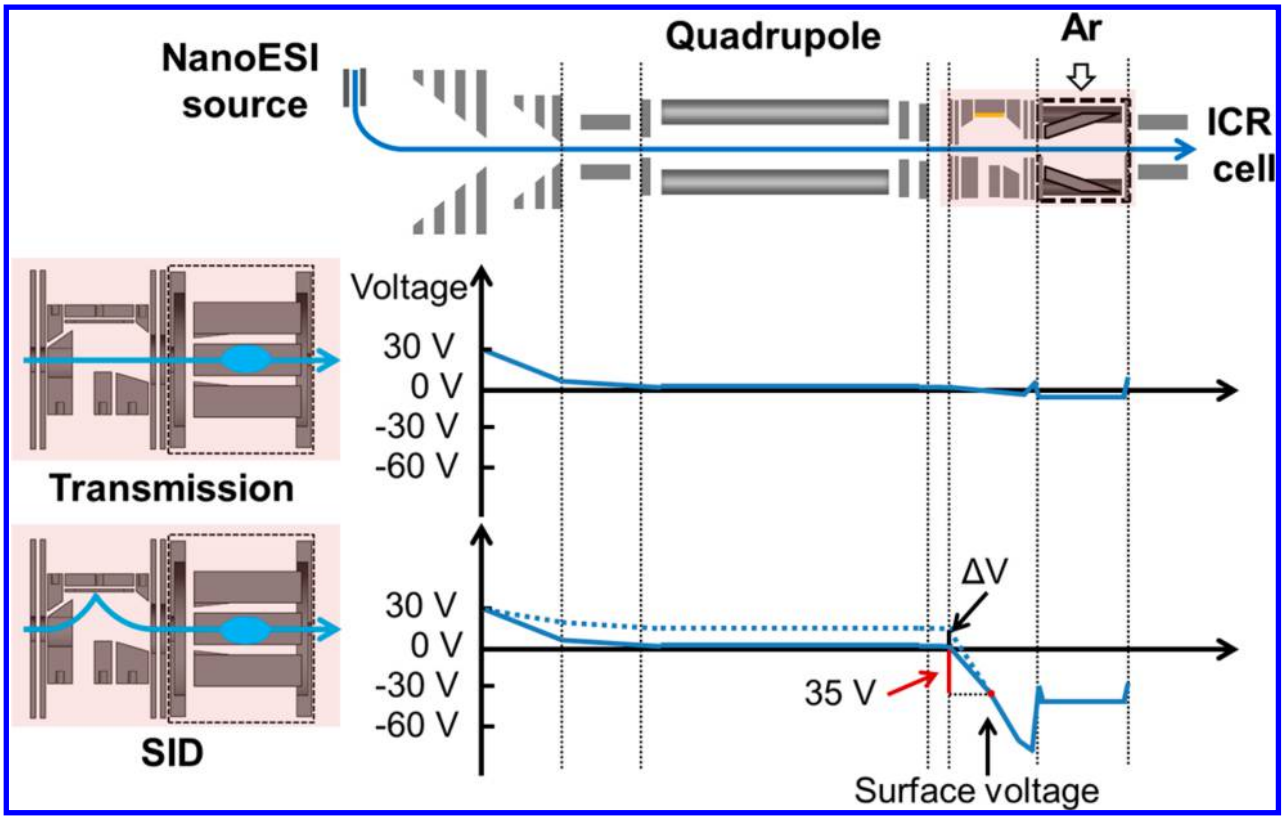

Figure 1. Schematics of a modified Bruker SolariX XR 15 T FT-ICR and its corresponding DC potentials applied for transmission mode (middle row) and SID mode (bottom row) in FT-ICR. The cutaway views of the SID device are highlighted in the shaded box on the left. In SID mode, the DC potential on the surface is −35 V (red dot), providing an acceleration voltage of 35 or 35 V + ΔV (as shown by the blue solid line and the blue dashed line). Product ions are accelerated through the SID exit lens and trapped and thermalized in the rectilinear quadrupole.

FT-ICR instruments.[8,21] However, CID of large protein complexes in the commercial collision cell in the Bruker FT-ICR platform is not highly efficient and can lead to loss of signal at the higher collision energies, which are required for dissociation of large protein complex ions.[22] SID has been applied in FT-ICR for studying the fragmentation of peptides in previous work,[23−28] but not for large protein complexes. In this study, an SID device was designed and installed in a hybrid FT-ICR instrument (15 T Bruker SolariX XR) external to the ICR Paracell. The SID-FT-ICR platform has been tested with several protein complex systems with distinct structures.

EXPERIMENTAL SECTION

SID Device. The SID device with a trapping region was designed to fit in place of the standard CID collision cell (Figure 1). The design of the SID region was optimized by SIMION 8.0 simulations. Protein complex ions with an initial kinetic energy from 50 to 100 eV at the entrance lens to the SID device were simulated in SIMION and accelerated to collision energies of approximately 500 eV. A kinetic energy retention of 10−20% after collision was considered.[16] Because dissociation of the precursor ions may happen between the surface and the exit lens of the SID device, generation of both precursors and fragments after surface collision was considered in the simulation. A script was written to change the kinetic energy of the precursor ions when they reach the surface and, for a portion of the ions, the SIMION mass and charge parameters were changed to representative fragment ion values. Collision with neutrals (gas) in the SID region was not considered in the program. The SID device consists of two parts, the SID region (2.75 cm in length) and the trap region (2.79 cm in length). There are ten DC electrodes in the SID region (Figure S1A). As shown in Figure S1D, the SID region has an open design to allow higher vacuum, minimizing collisions with background gas. The glass surface, coated with a 10 Å titanium layer and a 1000 Å gold layer, was further modified with a fluorinated self-assembled monolayer as previously described.[16] A rectilinear quadrupole with four asymptotic electrodes is enclosed in the trap region, which was filled with argon for collisional cooling. Nitrogen gas was also employed and the SID results were similar to the results obtained with argon (data not shown). RF and DC voltages were applied to the rectilinear quadrupole for trapping ions. DC voltages were applied to the asymptotic electrodes[29−31] for trapping and pulsing ions into the ICR cell. The SID electrodes were tuned to collide the ions with the surface electrode and the fragment ions were collected in the trap region after SID before being pulsed into the ICR cell for m/z detection (Figure 1). Initially, SIMION simulated tuning parameters were used to guide the tuning in the experiment and the experimental parameters were optimized to increase signal. The parameters listed in Table S1 in the Supporting Information are the optimized experimental tuning parameters after multiple iterations between experiment and SIMION. As with many MS experiments, the final tuning was optimized to best transmit a broad m/z range of ions.

Mass Spectrometer. All MS and MS/MS experiments were performed on a Bruker SolariX XR 15 T FT-ICR mass spectrometer (Bruker Daltonics, Bremen, Germany) with a customized SID device installed in the collision cell region,

DOI: 10.1021/acs.analchem.6b03986
Anal. Chem. 2017, 89, 895−901

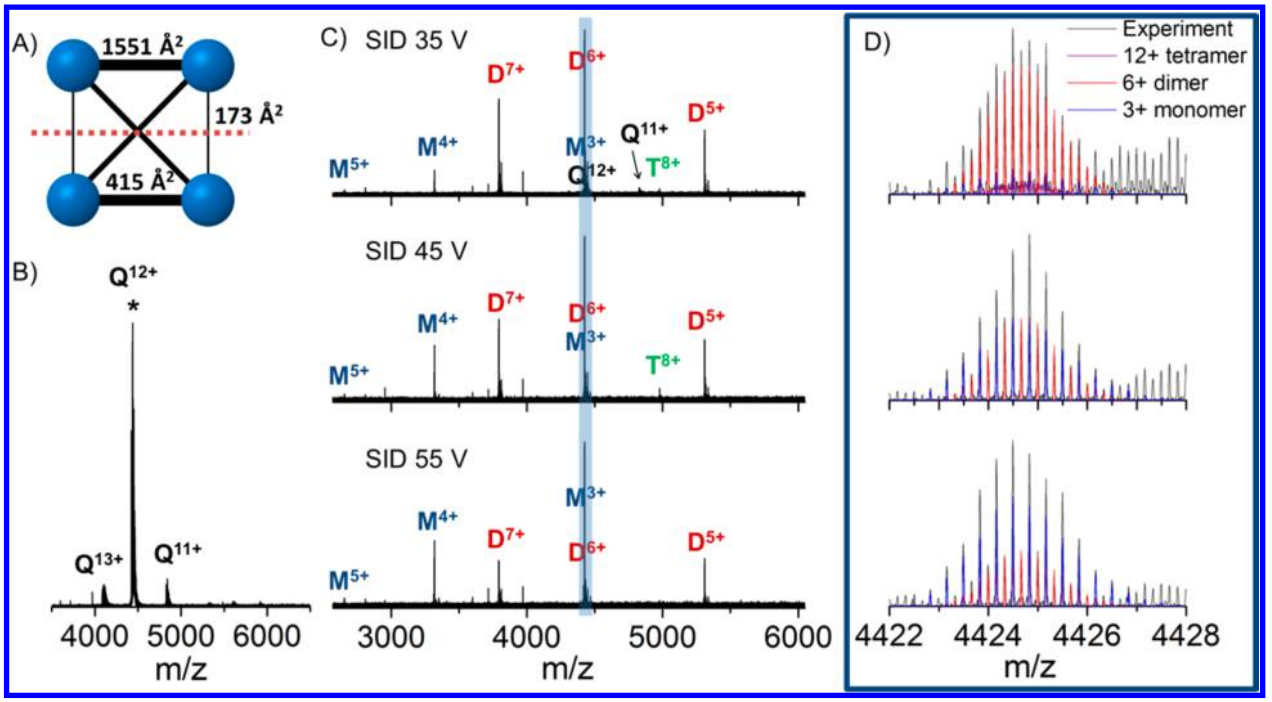

Figure 2. (A) Relative interactions between subunits in the streptavidin tetramer indicated by interaction surface areas. (B) Nanoelectrospray spray mass spectrum of 5 μM streptavidin tetramer in 100 mM EDDA by averaging 51 scans with a 4.6 s transient. The resolution of 12+ tetramer peaks is approximately 110000. (C) SID of the selected 12+ streptavidin tetramer at different SID acceleration voltages and (D) zoom in region of the peak highlighted in blue at different SID voltages. The SID spectra were acquired by averaging 50 scans with a 4.6 s transient. The resolution of peaks in zoom region is approximately 150000. The ratio of different species was scaled to reach the best match between the simulated data and experimental data. This is simplified by assigning a scaling factor to unique peaks that are contributed by only one species (e.g., 12+ tetramer has isotopic peaks that are not present for 6+ dimer and 3+ monomer). The experimental data are shown in gray lines, and the simulated isotopic distribution from different species are shown in purple (12+ tetramer), red (6+ dimer), and blue (3+ monomer).

replacing the original CID collision cell. All protein samples were ionized using a linear positioning station where the protein solution in a glass nanoelectrospray capillary is grounded through direct contact with a platinum wire.

Instrument settings in the Bruker FTICR control software used were as follows: in "Collision Cell" settings, the "Collision Voltage" was set to −4 V for transmission and −40 V for SID. The gas flow in the gas control settings was set to 80%. The "Time of Flight" between the gas collision cell and ICR cell varied from 1.2 to 1.8 ms depending on the protein system tested.

The DC potentials applied for transmission and SID are shown in Figure 1. The detailed SID tuning parameters are shown in Table S1. The SID acceleration voltage is defined as the voltage difference between the first entrance lens of the SID device (electrode 1 in Figure S1), which is similar to the voltage on the quadruople, and the surface (electrode 6 in Figure S1). Our research to date has shown that the SID device is capable of efficiently transmitting ions (small molecules, peptides, and protein complexes) with a broad range of m/z (from m/z 100 up to a 13.6 kDa, singly charged ion produced by MALDI). SID of high molecular weight protein complexes has not yet been optimized; precursor and product ions in this paper span m/z 1800−7100. In this first generation SID device, the collision cell in which SID products are trapped and thermalized is significantly shorter than the original collision cell. Typically, a 0.5 s accumulation time was used to obtain an MS spectrum with comparable signal to that obtained with the original collision cell with a 0.05 s accumulation time. Note that the short collision cell of the SID device was used by our MS facility for small molecule CID work, that is, no instrument modification was required to switch between SID of protein complexes and CID of small molecules. The MS and MS/MS data shown in this paper were acquired over a m/z range of 506−14000, regardless of precursor m/z. The spectra were acquired by averaging various numbers of scans to obtain isotopic distributions of all the peaks, including low intensity peaks. Because of the loss of precursor signal from quadrupole isolation, larger numbers of scans were used for MS/MS data acquisition.

Sample Preparation. Streptavidin (Thermo Pierce, Rockford, IL, U.S.A.), cholera toxin B (Sigma-Aldrich, St. Louis, MO, U.S.A.), and toyocamycin nitrile hydratase (obtained from Dr. Vahe Bandarian's lab, University of Utah),[32] which have all been characterized by SID in the QTOF platform previously,[33] were used to test dissociation with the SID device. The protein samples were buffer exchanged into 100 mM ethylenediammonium diacetate (EDDA, Sigma-Aldrich) with 6 kDa cutoff size exclusion chromatography spin columns (Bio-Rad). The final concentrations of buffer exchanged protein samples were confirmed with a Nanodrop 2000c spectrophotometer (Thermo Scientific, Wilmington, DE, U.S.A.). The samples were diluted to a protein complex concentration of 5 μM (streptavidin and toyocamycin nitrile hydratase) and 4 μM (cholera toxin B) for mass spectrometry analysis. The streptavidin/biotin complex was obtained by mixing the streptavidin sample with 500 μM biotin (Sigma- Aldrich) stock solution at a final concentration of 5 μM streptavidin tetramer and a ratio of streptavidin monomer/biotin 1:1.5.

DOI: 10.1021/acs.analchem.6b03986
Anal. Chem. 2017, 89, 895−901

The interfacial information for streptavidin (PDB ID: 1SWB) and cholera toxin B (PDB ID: 1FGB) were analyzed by PISA (Protein Interfaces, Surfaces and Assemblies)[34] to evaluate the theoretical SID fragmentation pathways.

RESULTS AND DISCUSSION

Streptavidin. Streptavidin is a dimer of dimers with relatively weak interactions between dimers. The interface areas between different streptavidin subunits are shown in Figure 2A. The streptavidin tetramer dissociates into highly charged monomers and low-charge trimers upon CID,[35] which is typical CID behavior where an unfolded monomeric subunit is ejected from the protein complex.[36,37] However, this CID pathway does not match the interface information from PISA analysis. On the other hand, the production of dimers from streptavidin tetramer in SID was found to be consistent with the magnitude of interface area.[14] A 4.6 s transient was used for mass analysis of streptavidin. The mass spectrum of streptavidin is shown in Figure 2B and the dominant peak corresponds to the 12+ streptavidin tetramer. The 12+ charge state ion of streptavidin tetramer was selected using the quadrupole (Figure 1) and fragmented via SID in the modified collision cell. The SID spectra of 12+ streptavidin tetramer ions at different acceleration voltages are shown in Figure 2C. All of the peaks are assigned with mass errors of less than 2 ppm. At an acceleration voltage of 35 V, the production of 7+, 6+, and 5+ dimers is dominant, which is consistent with breakage of the relatively weak interaction between dimers in a streptavidin tetramer. The symmetric dissociation of 12+ tetramers into dimers with around half of the original charge is the major pathway. Low intensities of 4+ and 5+ monomers and their complementary trimers can also be observed indicating the presence of a minor dissociation pathway. This result from SID in the FT-ICR is similar to the results previously obtained from a Q-TOF SID platform.[14] With an increase of acceleration voltage from 35 to 55 V (Figure 2C), the relative intensities of 3+ and 4+ monomers increase, while the relative intensities of 6+ and 7+ dimers decrease, indicating secondary fragmentation of dimers to monomers when higher internal energy is deposited by the surface collision process. For the SID spectra of 12+ streptavidin tetramer in Figure 2, the absolute intensity of the predominant peak at the m/z of 4425 (6+ dimer and 3+ monomer) is higher than the absolute intensity of the precursor peak when the data were acquired with the same number of scans, indicating that the trapping efficiency of the 12+ tetramer might be lower than that of 6+ dimer and 3+ monomer.

The peak at approximately m/z 4425, as highlighted in blue in Figure 2C, is the superposition of 12+ tetramer, 6+ dimer, and 3+ monomer, which have the same nominal mass but different isotopic distributions because of their different charge states. The zoom in region of the 4425 peak is shown in Figure 2D. Theoretical isotopic distributions of streptavidin oligomers were generated by the Simulation Pattern function in Bruker Compass DataAnalysis 4.2 software for comparison to the experimental data. Based on the sequence of streptavidin from its PDB file (PDB ID: 1SWB), the formula for streptavidin monomer, $C_{585}H_{883}N_{163}O_{192}$, was used to generate the theoretical isotope pattern of 3+ monomer, 6+ dimer and 12+ tetramer, for which the simulated data are shown in Figure 2D. At an SID acceleration voltage of 35 V, 6+ dimer (shown in red) is the dominant species. The increase of the relative intensity of 3+ monomer with increasing SID collision voltage can be clearly observed from the change of isotopic distribution.

The streptavidin−biotin complex was also analyzed by SID (Figure S2). The streptavidin subunit with and without the N-terminal methionine (Met) can be distinguished (Figure 3A),

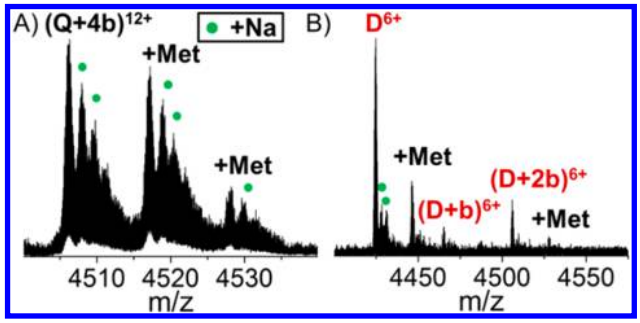

Figure 3. (A) Zoom in spectrum of 12+ streptavidin−biotin tetramer. The spectrum was acquired by averaging 100 scans with a 4.6 s transient. The resolution of 12+ tetramer peaks is approximately 120000. "b" represents biotin. Part of the streptavidin monomers within the tetramer have an extra methionine at the N-terminus, thus giving rise to the extra distribution(s) of peaks. (B) Zoom-in spectrum of the 6+ dimer produced from SID of 12+ streptavidin−biotin tetramer (within m/z range 4520 ± 50) at an acceleration voltage of 35 V. The spectrum was acquired by averaging 200 scans with a 4.6 s transient.

along with varying degrees of sodium adduction. The sodium adducts and biotins bound to the streptavidin dimer can also be clearly assigned from the SID spectrum based on their corresponding isotopic distributions (Figures 3B and S3). The relative intensity of nonspecific adducts (e.g., sodium) on the dimer is much lower than that on the tetramer (Q + 4b), indicating the loss of nonspecific adducts during the SID process. The biotin on the streptavidin dimer demonstrates that some dimers generated from the tetramer preserve their folded structure and the ligand. The ultrahigh resolution of the FT-ICR allows these ligand bound and modified species with relatively small mass differences to be easily resolved and characterized.

Cholera Toxin B (CTB). In contrast with the structure of streptavidin as a dimer of dimers, cholera toxin B (CTB) is a ring structured homopentamer (see in the inset of Figure 4A). As shown in Figure 4A, the dominant peak in the nano-electrospray MS of CTB is the peak from the 13+ CTB pentamer. The SID spectrum of 13+ CTB pentamer ions at an acceleration voltage of 35 V shows the production of monomers, dimers, trimers, and tetramers (Figure 4B), which is similar to the previous result obtained on a Q-TOF instrument.[38] There are similar interactions between each pair of monomers in the ring structure of CTB pentamer. As such, theoretically, the formation of CTB monomer, dimer, trimer, and tetramers is ∼equally likely by cleaving two interfaces in the cyclic pentamer (the inset of Figure 4).

The overlapping of 2+ monomer, 4+ dimer, 6+ trimer, and 8+ tetramer can be well-distinguished based on the isotopic distribution of each species (Figure 4D). The formula of CTB monomer, $C_{511}H_{816}N_{142}O_{156}S_5$, was obtained from the PDB file (PDB ID: 1FGB) and used to simulate the theoretical isotopic pattern of CTB (Figure 4C). The isotopic peaks are well-resolved and the resolution for the peaks in the zoomed in region is greater than 200000 with a 9.2 s transient at around

DOI: 10.1021/acs.analchem.6b03986
Anal. Chem. 2017, 89, 895−901

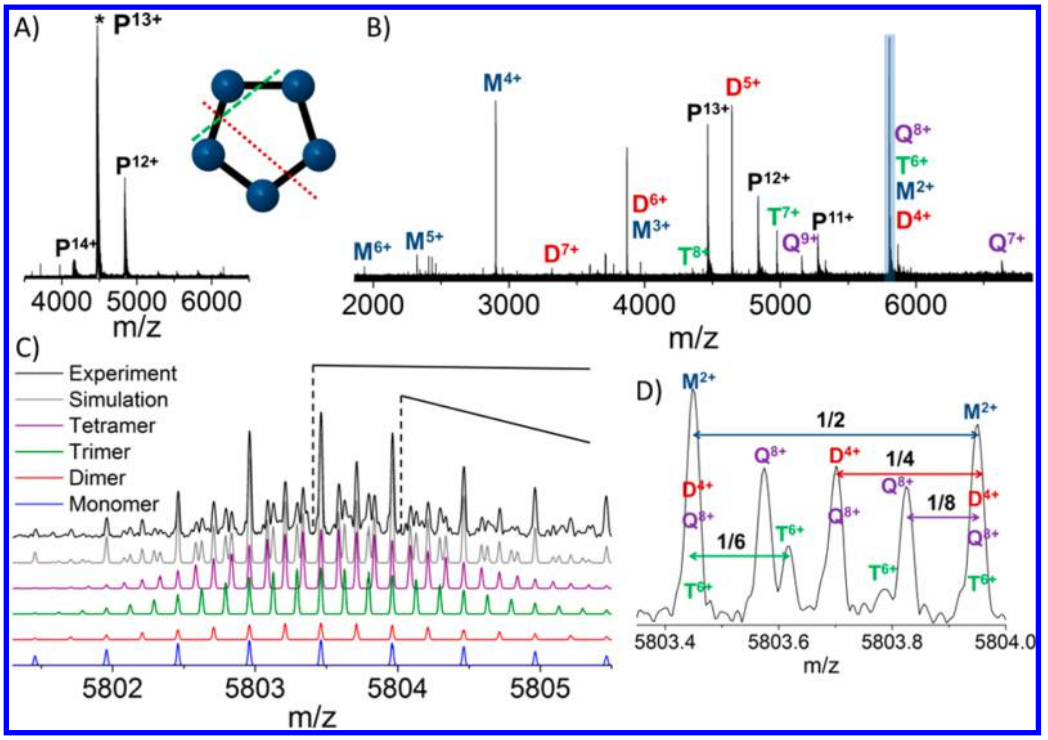

Figure 4. (A) Nanoelectrospray mass spectrum of 4 μM CTB pentamer in 100 mM EDDA. The 13+ CTB pentamer was selected for SID. Inset: connectivity between subunits in CTB. The spectrum was acquired by averaging 30 scans with a 4.6 s transient. The resolution of 13+ pentamer peaks is approximately 130000. (B) SID of 13+ CTB pentamer at an SID acceleration voltage of 35 V. The spectrum was acquired by averaging 181 scans with a 9.2 s transient. (C) Zoomed-in region showing the peak highlighted in blue in (B). The experimental data are shown with black lines and the simulated isotopic distributions from different species are shown in purple (8+ tetramer), green (6+ trimer), red (4+ dimer), blue (2+ monomer), and gray (sum of all speices). (D) Further zoom in of m/z around 5803.7. The resolution of peaks is approximately 210000.

m/z 5803.7 (Figure 4D). The mass errors are within 2.2 ppm and the simulated isotopic peaks are well-aligned with the peaks from the experimental data, indicating the ultrahigh resolution and high mass accuracy.

Toyocamycin Nitrile Hydratase (TNH). TNH is a heterohexamer with three different subunits α, β, and γ. Its structural model has been developed based on multiple mass spectrometry techniques, including SID results from a Q-IM-TOF instrument (Figure S4).[33] The model shows that TNH is a dimer of trimers with relatively weak interaction(s) between the two trimers. There is one copy of the α, β, and γ subunits in each of the trimers. Within each of the trimers, the strongest interaction is the interaction between the α and β subunits. TNH was tested on the SID-FT-ICR platform with a 9.2 s transient. The nanoelectrospray mass spectrum of TNH (Figure 5A) displays the 15+ hexamer charge state as the dominant peak. Because the upper m/z selection limitation of the quadrupole is at roughly m/z 6000 in this instrument, the selection window was left relatively wide. Three TNH hexamer charge states (16+, 15+, and 14+) are included in the selection (highlighted in Figure 5A).

The SID spectrum of TNH hexamer at an acceleration voltage of 45 V is shown in Figure 5B. The fragment peaks can be isotopically resolved such that the charge state can be assigned with mass errors within 1.5 ppm. The SID result shows that the $\alpha\beta\gamma$ trimers are the major products with 8+ and 7+ as the dominant charge states which are around half of the precursor charge state (15+ dominant). This result agrees with the previous conclusion that TNH is a dimer of trimers. In addition, the minor products, $\alpha\beta$ dimers and their complementary $\alpha\beta\gamma_2$ tetramers, can be observed which matches well with the strong interactions between α and β subunits in the structural model developed previously.[33] In the zoom-in region of the 6+ α subunit SID product (Figure 5C), α subunits both with and without a cobalt and three additional cysteine−sulfenate oxygens[32] can be well-distinguished. There are three cysteines in the sequence of the α subunit. The formula of α, $C_{931}H_{1501}N_{271}O_{277}S_5$, with one disulfide bond formed was used to generate the isotopic distribution of α subunit without Co^{2+} and sulfenic acid oxygens (purple line in Figure 5D). The formula $C_{931}H_{1501}N_{271}O_{280}S_5Co$, with the disulfide bond reduced, Co^{2+} replacing two protons, and three additional cysteine−sulfenate oxygens, was used to generate the isotopic distribution of α subunit with a cobalt and three oxygens (red line in Figure 5D). The simulated isotopic peaks are well-aligned with the peaks from the experimental data, showing the presence of α in two forms, disulfide bond oxidized without a cobalt and three oxygens, and disulfide bond reduced with a cobalt and three oxygens. This is further confirmed by the observation that the mixture of α subunits with and without a cobalt and three oxygens can be found in all α containing fragments (Figure S5).

CONCLUSIONS

SID has been successfully implemented external to the ICR cell in a hybrid 15 T Bruker SolariX XR FT-ICR instrument by replacing the standard CID collision cell with the SID device. The SID device can be used for conventional ion transmission and surface collisions. Ions, including small molecules, peptides, and protein complexes, with m/z ranges of 100−14000 have been transmitted and detected with the SID device installed. Protein complex systems with different structures (home-

DOI: 10.1021/acs.analchem.6b03986
Anal. Chem. 2017, 89, 895−901

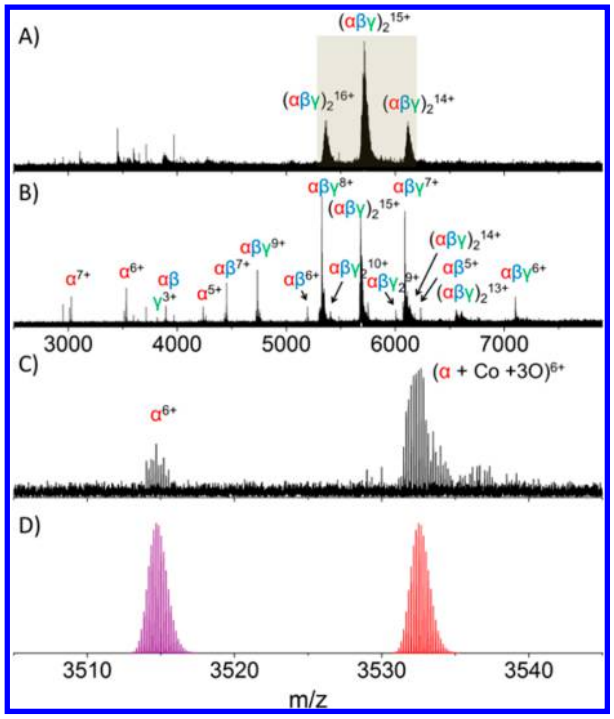

Figure 5. (A) Mass spectrum of 5 μM TNH hexamer in 100 mM EDDA. The spectrum was acquired by averaging 50 scans with a 9.2 s transient. The resolution of 15+ hexamer peaks is approximately 200000. The hexamer peaks in the highlighted region were selected and (B) dissociated with SID at an acceleration voltage of 45 V. The spectrum was acquired by averaging 255 scans with a 9.2 s transient. (C) Zoom-in region of 6+ charge state of the α subunit in the SID spectrum. (D) The simulated isotopic distributions of the 6+ charge state of the α subunit with (red) and without (purple) a cobalt and three additional oxygens.

tetramer, homopentamer, and heterohexamer) were successfully fragmented after collision with a modified surface and their FT-ICR product ratios match well with the SID results obtained previously from the Q-TOF platform. Ultrahigh mass resolution in the FT-ICR makes it possible to differentiate overlapping species with the same nominal m/z but different oligomeric and charge states by resolution of their isotopic distributions. In addition, peaks corresponding to the addition of metal cations and ligands can also be isotopically resolved. The SID-FT-ICR platform has the potential to characterize heterogeneous samples and protein–ligand interactions with minor mass differences. The SID device is currently being tested with more protein complexes to optimize the ion transmission and the SID design in our laboratory.

■ ASSOCIATED CONTENT

Supporting Information

The Supporting Information is available free of charge on the ACS Publications website at DOI: 10.1021/acs.analchem.6b03986.

The detailed SID model and tuning parameters for the SID experiments. The MS and SID spectra of streptavidin–biotin. The zoom in spectra of streptavidin–biotin dimer and tetramer, and TNH $\alpha\beta$ dimer and $\alpha\beta\gamma$ trimer, and their corresponding theoretical isotopic distributions. The SID spectrum of 15+ TNH hexamer acquired in a Q-TOF instrument (PDF).

■ AUTHOR INFORMATION

Corresponding Author

*Tel.: +1 614 292 8687. E-mail: wysocki.11@osu.edu.

ORCID

Jing Yan: 0000-0001-9901-5656

Author Contributions

The manuscript was written by J.Y. with contributions to experiment design and writing from all authors.

Notes

The authors declare no competing financial interest.

■ ACKNOWLEDGMENTS

The authors acknowledge Dr. Micah T. Nelp and Dr. Vahe Bandarian from the University of Utah for kindly providing the TNH sample. The project is supported by the National Science Foundation (NSF DBI 1455654) and NIH (1S10OD018507; ICR purchase). A portion of the research was funded by EMSL, a DOE Office of Science User Facility sponsored by the Office of Biological and Environmental Research and located at Pacific Northwest National Laboratory.

■ REFERENCES

(1) Spirin, V.; Mirny, L. *Proc. Natl. Acad. Sci. U. S. A.* **2003**, *100*, 12123–12128.
(2) Robinson, C. V.; Sali, A.; Baumeister, W. *Nature* **2007**, *450*, 973–982.
(3) Sharon, M. *J. Am. Soc. Mass Spectrom.* **2010**, *21*, 487–500.
(4) Loo, J. A. *Int. J. Mass Spectrom.* **2000**, *200*, 175–186.
(5) Heck, A. J. R. *Nat. Methods* **2008**, *5*, 927–933.
(6) Benesch, J. L. P.; Robinson, C. V. *Curr. Opin. Struct. Biol.* **2006**, *16*, 245–251.
(7) Lermyte, F.; Konijnenberg, A.; Williams, J. P.; Brown, J. M.; Valkenborg, D.; Sobott, F. *J. Am. Soc. Mass Spectrom.* **2014**, *25*, 343–350.
(8) Li, H.; Wolff, J. J.; Van Orden, S. L.; Loo, J. A. *Anal. Chem.* **2014**, *86*, 317–320.
(9) Zhou, M.; Wysocki, V. H. *Acc. Chem. Res.* **2014**, *47*, 1010–1018.
(10) Morrison, L. J.; Brodbelt, J. S. *J. Am. Chem. Soc.* **2016**, *138*, 10849–10859.
(11) Tamara, S.; Dyachenko, A.; Fort, K. L.; Makarov, A. A.; Scheltema, R. A.; Heck, A. J. R. *J. Am. Chem. Soc.* **2016**, *138*, 10860–10868.
(12) Benesch, J. L. P.; Aquilina, J. A.; Ruotolo, B. T.; Sobott, F.; Robinson, C. V. *Chem. Biol.* **2006**, *13*, 597–605.
(13) Brodbelt, J. S. *Anal. Chem.* **2016**, *88*, 30–51.
(14) Quintyn, R. S.; Yan, J.; Wysocki, V. H. *Chem. Biol.* **2015**, *22*, 583–592.
(15) Quintyn, R. S.; Zhou, M.; Yan, J.; Wysocki, V. H. *Anal. Chem.* **2015**, *87*, 11879–11886.
(16) Galhena, A. S.; Dagan, S.; Jones, C. M.; Beardsley, R. L.; Wysocki, V. H. *Anal. Chem.* **2008**, *80*, 1425–1436.
(17) Zhou, M.; Huang, C.; Wysocki, V. H. *Anal. Chem.* **2012**, *84*, 6016–6023.
(18) Lössl, P.; Snijder, J.; Heck, A. R. *J. Am. Soc. Mass Spectrom.* **2014**, *25*, 906–917.
(19) Boldin, I. A.; Nikolaev, E. N. *Rapid Commun. Mass Spectrom.* **2011**, *25*, 122–126.
(20) Nikolaev, E. N.; Boldin, I. A.; Jertz, R.; Baykut, G. *J. Am. Soc. Mass Spectrom.* **2011**, *22*, 1125–1133.
(21) Nikolaev, E. N.; Vladimirov, G. N.; Jertz, R.; Baykut, G. *Mass Spectrom.* **2013**, *2*, S0010.
(22) Wen, J.; Zhang, H.; Gross, M. L.; Blankenship, R. E. *Biochemistry* **2011**, *50*, 3502–3511.
(23) Laskin, J.; Denisov, E. V.; Shukla, A. K.; Barlow, S. E.; Futrell, J. H. *Anal. Chem.* **2002**, *74*, 3255–3261.

DOI: 10.1021/acs.analchem.6b03986
Anal. Chem. 2017, 89, 895–901

(24) Laskin, J.; Futrell, J. H. *J. Am. Soc. Mass Spectrom.* **2003**, *14*, 1340−1347.
(25) Fernandez, F. M.; Wysocki, V. H.; Futrell, J. H.; Laskin, J. *J. Am. Soc. Mass Spectrom.* **2006**, *17*, 700−709.
(26) Williams, E. R.; Henry, K. D.; McLafferty, F. W.; Shabanowitz, J.; Hunt, D. F. *J. Am. Soc. Mass Spectrom.* **1990**, *1*, 413−416.
(27) Castoro, J. A.; Wilkins, C. L.; Woods, A. S.; Cotter, R. J. *J. Mass Spectrom.* **1995**, *30*, 94−98.
(28) Tsaprailis, G.; Nair, H.; Somogyi, Á.; Wysocki, V. H.; Zhong, W.; Futrell, J. H.; Summerfield, S. G.; Gaskell, S. J. *J. Am. Chem. Soc.* **1999**, *121*, 5142−5154.
(29) Wilcox, B. E.; Hendrickson, C. L.; Marshall, A. G. *J. Am. Soc. Mass Spectrom.* **2002**, *13*, 1304−1312.
(30) Loboda, A.; Krutchinsky, A.; Loboda, O.; McNabb, J.; Spicer, V.; Ens, W.; Standing, K. *Eur. Mass Spectrom.* **2000**, *6*, 531−536.
(31) Mansoori, B. A.; Dyer, E. W.; Lock, C. M.; Bateman, K.; Boyd, R. K.; Thomson, B. A. *J. Am. Soc. Mass Spectrom.* **1998**, *9*, 775−788.
(32) Nelp, M. T.; Astashkin, A. V.; Breci, L. A.; McCarty, R. M.; Bandarian, V. *Biochemistry* **2014**, *53*, 3990−3994.
(33) Song, Y.; Nelp, M. T.; Bandarian, V.; Wysocki, V. H. *ACS Cent. Sci.* **2015**, *1*, 477−487.
(34) Krissinel, E.; Henrick, K. *J. Mol. Biol.* **2007**, *372*, 774−797.
(35) Schwartz, B. L.; Bruce, J. E.; Anderson, G. A.; Hofstadler, S. A.; Rockwood, A. L.; Smith, R. D.; Chilkoti, A.; Stayton, P. S. *J. Am. Soc. Mass Spectrom.* **1995**, *6*, 459−465.
(36) Hall, Z.; Hernández, H.; Marsh, J. A.; Teichmann, S. A.; Robinson, C. V. *Structure* **2013**, *21*, 1325−1337.
(37) Popa, V.; Trecroce, D. A.; McAllister, R. G.; Konermann, L. *J. Phys. Chem. B* **2016**, *120*, 5114−5124.
(38) Ju, Y.; Quintyn, R. S.; Busch, F.; Yan, J. Y.; Wysocki, V. H. 2016, Submitted for publication.

DOI: 10.1021/acs.analchem.6b03986
Anal. Chem. 2017, 89, 895−901